ChemComm

Accepted Manuscript

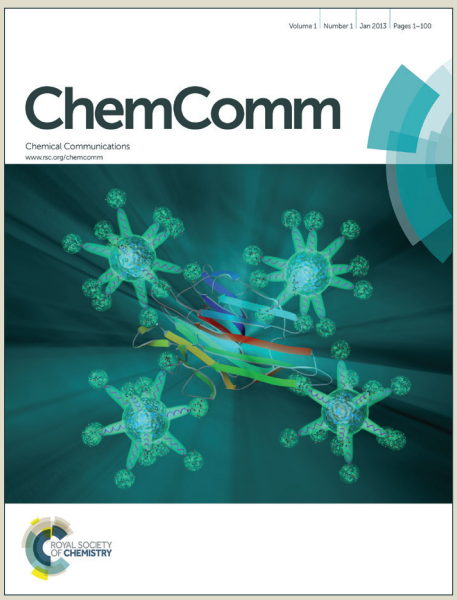

ROYAL SOCIETY OF CHEMISTRY

www.rsc.org/chemcomm

Cite this: DOI: 10.1039/c0xx00000x

www.rsc.org/xxxxxx

ARTICLE TYPE

Cu_2O Template Synthesis of High-Performance PtCu Alloy Yolk-Shell Cube Catalysts for Direct Methanol Fuel Cells

Sheng-Hua Ye, Xu-Jun He, Liang-Xin Ding, Zheng-Wei Pan, Ye-Xiang Tong, Mingmei Wu,* and Gao-Ren Li*

Received (in XXX, XXX) Xth XXXXXXXXX 20XX, Accepted Xth XXXXXXXXX 20XX

DOI: 10.1039/b000000x

Novel PtCu alloy yolk-shell cubes were fabricated via the disproportionation and displacement reactions in Cu_2O yolk-shell cubes, and they exhibit significantly improved catalytic activity and durability for methanol electrooxidation.

Fuel cells have attracted great interest as they are promising candidates for providing clean energy.[1-5] Over the past decades, extensive research has been devoted to the development of direct methanol fuel cells (DMFCs) that have been regarded as the promising future power sources, especially for mobile and portable applications.[6-8] However, the major challenges in this field lie in the insufficient activity, unsatisfied durability and high cost of Pt catalysts. These limitations inevitably lead to a low operating efficiency of the fuel cells, which highlights the need of low cost and high active and durable catalysts.[9-11]

To address the above limitations, recently much attention have been focused on the synthesis of Pt-M bimetallic electrocatalysts (where M=Fe, Co, Ni, Cu, etc.).[12-15] Owing to the synergistic effects between two metals, the bimetallic Pt-M catalysts often display low cost and superior catalytic performance compared to pure Pt catalysts. For example, the bimetallic PtCu alloy catalysts possess high catalytic activity and superior CO tolerance toward methanol electrooxidation in comparison with pure Pt catalysts, and has been considered as a promising candidate catalyst for DMFCs.[21] On the other hand, it is also realized that the surface shape and crystal structure of nanocrystals play a significant role in the electrocatalytic activity and durability.[22-27] In order to further minimize the use of precious metals without sacrificing the catalytic performance, it is therefore interesting to "transfer" the idea of shape-controlled Pt crystals into its binary system. Recently, the yolk-shelled structures have attracted much interest because of their unique properties and the special core@void@shell structure.[28-29] Compared with traditional core-shell structure, the yolk-shell structures possess higher surface area, larger void space and lower density, which leads to their wide applications in drug delivery, lithium-ion batteries and catalysis.[30-32] The catalysts with yolk-shell structures will possess following advantages: (*i*) The outer shells can effectively hinder aggregation of neighbouring particles, even under the harsh experimental conditions. (*ii*) The interstitial hollow space can allow the electroactive species to fully touch catalyst and enhance the utilization ratio of catalyst. (*iii*) The inner cores can afford more exposed active sites, which in turn provide much more effective interactions with the electroactive species. Therefore, by combining the merits of bimetallic system and yolk-shell structures, it is expected that the novel electrocatalysts with low-cost and high catalytic activity and durability could be designed and fabricated.

Herein, we develop novel bimetallic PtCu alloy yolk-shell cube catalysts for methanol electrooxidation by using Cu_2O yolk-shelled cubes as templates. The Cu_2O yolk-shelled cubes were firstly reported in this study, and they were fabricated by combing ZnO-assisted electrodeposition with Ostwald ripening. The formation mechanism of Cu_2O yolk-shelled cubes is detailedly investigated in this study as it is an important p-type semiconductor material and has aroused many interests because of their potential applications in solar energy conversion, catalysis, gas sensor, and so forth. Then PtCu alloy yolk-shell cubes were synthesized via disproportionation and displacement reactions in the Cu_2O yolk-shell cubes. According to the previous reports, the crystals with yolk-shell structures are usually spherical, and the yolk-

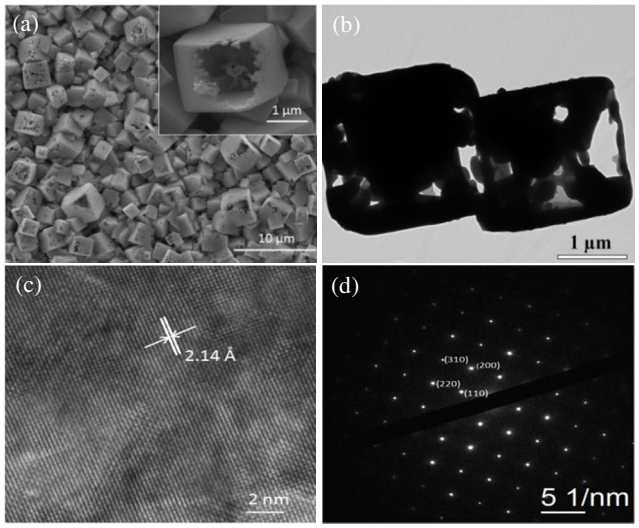

Figure 1. (a) SEM, (b) TEM, (c) HRTEM and (d) SAED images of Cu_2O yolk-shell cubes (inset in (a) is SEM image of a broken Cu_2O cube).

MOE Laboratory of Bioinorganic and Synthetic Chemistry/KLGHEI of Environment and Energy Chemistry/ School of Chemistry and Chemical Engineering, Sun Yat-sen University, Guangzhou 510275, China
Fax: 86-20-84112245; Tel: 86-20-84110071
E-mail: ligaoren@mail.sysu.edu.cn

† Electronic supplementary information (ESI) available. See DOI: 10.1039/XXXXXXXX

shell cubes were rarely reported.[33-35] Compared with spherical morphology, the cubes will exhibit many unique physical and chemical characteristics because the regular crystal planes can show different surface atomic structures and surface energies.[36] Here these fabricated PtCu alloy yolk-shell cubes exhibit much improved electrocatalytic activity and durability compared with commercial Pt/C catalysts.

The details of the fabrication of Cu_2O yolk-shell cubes are described in the experimental section in Supporting Information. SEM image of the Cu_2O yolk-shell cubes is shown in Figure 1a, which shows the sizes of Cu_2O cubes are 2.0~5.0 μm. The inset in Figure 1a shows a broken Cu_2O yolk-shell cube. A typical TEM image is shown in Figure 1b, which shows Cu_2O cubes have yolk-shell structures. The sizes of inner cores are 0.5~1.0 μm and the shell thicknesses are 100~200 nm. HRTEM image and SAED pattern of Cu_2O cubes were shown in Figure 1c and 1d, respectively, which confirms the single-crystal structure of Cu_2O. XRD of Cu_2O yolk-shell cubes is shown in Figure 2a. The (110), (111), (200), (220), and (311) reflections of Cu_2O are seen, and these diffraction peaks can be exclusively indexed to the cubic phase of Cu_2O (JCPDS #05-0667). Other peaks come from the substrate. No peak of Cu, CuO, $Cu(OH)_2$ or other impurities is detected in the XRD pattern, confirming high purity of the Cu_2O yolk-shell cubes.

Before deposition of Cu_2O, a thin layer of ZnO is deposited on the surface of Ti substrate as shown in Figure S1. Here ZnO layer is crucial for the formation of Cu_2O cubes. We successfully realized the fabrication of Cu_2O yolk-shell cubes by ZnO-induced electrodeposition combined with ostwald ripening. The electrochemical formation process of Cu_2O is suggested as following. Firstly, Cu^{2+} ions are reduced to Cu^+ ions on cathode, and then OH^- ions in solution will react with Cu^+ ions to form Cu_2O. These processes can be expressed as following equation (1).

$$2Cu^{2+}+2e^{-}+2OH^{-}\rightarrow Cu_2O+H_2O \quad (1)$$

$$Cu_2O+2OH^{-}\rightarrow 2CuO+H_2O+e^{-} \quad (2)$$

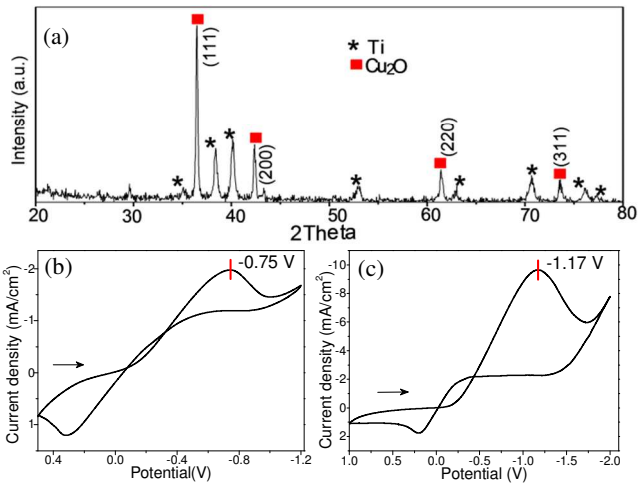

Figure 2. (a) XRD pattern of the Cu_2O yolk-shell cubes. CVs of different electrodes of (b) ZnO/Ti and (c) Ti in solution of 0.02 M $CuCl_2$+0.68 mM $C_6H_5Na_3O_7{\cdot}2H_2O$ at 20 mV/s.

The role of ZnO layer is studied by cyclic voltammograms (CVs) measured on ZnO/Ti and Ti electrodes in the solution of 0.02 M $CuCl_2$+0.68 mM/L $C_6H_5Na_3O_7{\cdot}2H_2O$ as shown in Figure 2b and 2c, respectively. In Figure 2b, one reduction wave at -0.75 V is seen, and this wave corresponds to the formation of Cu_2O via reaction (1). When potential is scanned positively, one oxidation wave is seen, and this wave corresponds to the oxidation of Cu_2O to form CuO via reaction (2). Herein, compared with that on Ti electrode (Figure 2b), the CV measured on ZnO/Ti electrode shows the reduction wave is positively shift, indicating that the ZnO layer can obviously induce the electroreduction of Cu^{2+} to form Cu_2O. In addition, the conductivity of ZnO is much poorer than that of metal Ti and this will lead to slower electrodeposition rate of Cu_2O. Compared with CVs measured on ZnO/Ti and Ti electrodes (Figure 2b and 2c), the peak current density of reduction wave on ZnO/Ti is much smaller than that on Ti, indicating that the growth rate of Cu_2O on ZnO layer is much smaller than that on Ti substrate. Accordingly, the slow growth rate is highly propitious to the formation of well-defined regular Cu_2O cubes as shown in Figure S2a. However, when the electrodeposition rate is carried out on Ti substrate, hollow Cu_2O cubes were not fabricated and only the Cu_2O nanosheets were obtained as shown in Figure S2b. Therefore, the above results demonstrate the crucial role of ZnO layer for the fabrication of Cu_2O yolk-shell cubes by electrodeposition.

Using Cu_2O yolk-shell cubes as templates, we successfully realized the synthesis of novel bimetallic PtCu alloy yolk-shell cube catalysts for methanol electrooxidation. On account of the facts that the disproportionation reaction of Cu_2O can be occurred in acid solution and the reducing potential of Cu^{2+}/Cu pairs (0.337 V) is much lower than that of $PtCl_6^{2-}$/Pt (0.735 V), we successfully fabricate PtCu alloy yolk-shell cubes by using disproportionation reaction and galvanic displacement in the Cu_2O yolk-shell cubes. The reactions for the formation of PtCu alloys are listed as following:

$$Cu_2O + 2H^+ \rightarrow Cu + Cu^{2+} + H_2O \quad (3)$$

$$2Cu + PtCl_6^{2-} \rightarrow Pt + 2Cu^{2+} + 6Cl^- \quad (4)$$

$$Pt+Cu \rightarrow PtCu\ alloys \quad (5)$$

SEM and TEM images of PtCu alloy yolk-shell cubes are shown in Figure 3a and 3b, respectively, which shows the existence of yolk-shell cubes. HRTEM image and SAED pattern in Figure 3c and 4d indicate the polycrystalline structure of the PtCu yolk-shell cubes. The composition of PtCu yolk-shell cubes is determined by ICP-AES and the ratio of Pt/Cu is ~1.07. XRD pattern of PtCu yolk-shell cubes is shown in the Figure 4a. The diffraction peaks of Cu_2O disappear and there isn't any Pt or Cu diffraction peak. Two broad diffraction peaks at 2θ=40.8^0 and 47.6^0 can be indexed to (111) and (200) planes of PtCu alloy, respectively (JCPDS #48-1549), indicating the formation of PtCu alloys.

Electrochemically active surface area (ECSA) of the catalysts are studied and Figure 4b shows cyclic voltammograms (CVs) of PtCu alloy yolk-shell cubes and commercial Pt/C catalysts in a N_2 purged 0.5 M H_2SO_4 solution at a scan rate of 20 mV/s. In the CV of Pt/C catalyst, hydrogen desorption/adsorption peaks and Pt oxidation/reduction peaks were clearly seen. Accordingly, in the CV of PtCu alloy yolk-shell cubes, besides hydrogen desorption/adsorption peaks and Pt oxidation/reduction peaks, Cu oxidation/reduction peaks were seen, indicating the existence of PtCu alloys. The ECSA of catalyst is calculated from the area of hydrogen desorption after deduction of double-layer region according to the equation[37] ECSA=$Q_H/(210\times W_{Pt})$, where W_{Pt} represents the Pt loading ($\mu g/cm^2$) on electrode, Q_H is the total charge (μC) for

hydrogen desorption, and 210 represents the charge ($\mu C/cm^{-2}_{Pt}$) required to formation or stripping of a hydrogen monolayer. Herein, the calculated ECSA of PtCu alloy yolk-shell cubes is 116 m^2 (g Pt)$^{-1}$, and the Pt/C catalyst is 69 m^2 (g Pt)$^{-1}$. Therefore, the PtCu alloy yolk-shell cubes show larger ECSA than the commercial Pt/C catalysts.

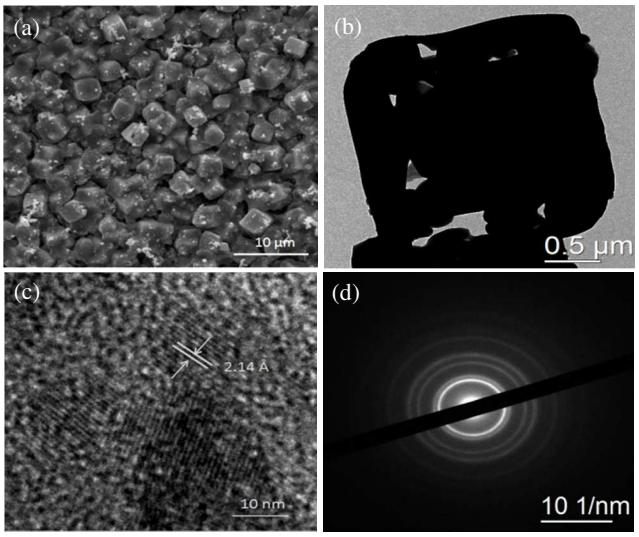

Figure 3. (a) SEM, (b) TEM, (c) HRTEM and (d) SAED pattern of PtCu alloy yolk-shell cubes that are fabricated from Cu_2O yolk-shell cubes.

The catalytic performance of PtCu Alloy yolk-shell cubes toward methanol oxidation was studied in solution of 0.5 M CH_3OH + 0.5 M H_2SO_4 and the result is shown in Figure 4c, which shows the specific peak current density (all are normalized to the ECSA) of PtCu alloy yolk-shell cubes was almost 2.5 times higher than that of commercial Pt/C, indicating the specific catalytic activity of the PtCu alloy yolk-shell cubes is much higher than that of commercial Pt/C catalysts. In addition, the onset potential of backward scan peak of PtCu alloy yolk-shell cubes obviously shifts positively relative to that of Pt/C catalyst as shown in Figure 4c. It is well known that the backward anodic peak is attributed to the continuous oxidation of incompletely oxidized carbonaceous intermediates, such as CO, $HCOO^-$, and HCO^-, accumulated on the surfaces of catalysts during methanol oxidation.[38] Therefore, the positive shift of onset potential of backward scan peak suggests the weakened chemisorption of intermediate species on PtCu alloy yolk-shell cubes, which will facilitate the removal of adsorbed intermediate species to generate clean and active surface sites and accordingly will enhance electroactivity and durability of PtCu alloy yolk-shell cubes. In addition, it is worth to noting that the difference potential between the forward peak and backward peak of PtCu alloy yolk-shell cubes is only 0.16 V, which is smaller than that of commercial Pt/C catalyst (0.21 V). This implies that the Pt atoms in PtCu alloy yolk-shell cubes can be easier refreshed compared with those in commercial Pt/C catalysts.

In order to further evaluate the rate of surface poisoning of PtCu alloy yolk-shell cubes, the chronoamperometry curves of catalysts were measured in solution of 0.5 M CH_3OH + 0.5 M H_2SO_4 as shown in Figure 4d. The potential was held at 0.75 V during the measurements. It is obvious that the PtCu alloy yolk-shell cubes exhibit a much higher current density over time and a much slower attenuation in comparison with the commercial Pt/C catalysts, indicating a much higher catalytic activity for methanol electro-oxidation and a much higher tolerance to the carbonaceous species generated during methanol oxidation.

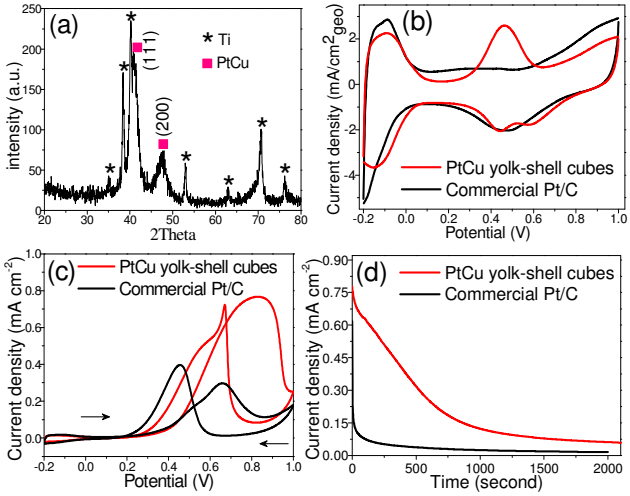

Figure 4. (a) XRD pattern of PtCu alloy yolk-shell cubes; (b) CVs of PtCu alloy yolk-shell cubes and commercial Pt/C in solution of 0.5 M H_2SO_4 at 20 mV/s; (c) CVs of PtCu alloy yolk-shell cubes and commercial Pt/C in solution of 0.5 M CH_3OH+0.5 M H_2SO_4 at 20 mV/s; (d) Chronoamperometry curves of PtCu alloy yolk-shell cubes and commercial Pt/C in solution of 0.5 M H_2SO_4+0.5 M CH_3OH at 0.75 V.

Conclusions

In summary, we have developed the synthesis of novel Cu_2O yolk-shell cube templates and their application for the synthesis of PtCu alloy yolk-shell cube catalysts that own abundant active sites, short diffusion lengths of active species and sufficient void space to buffer volume expansion. When tested as catalysts for methanol electrooxidation, the fabricated PtCu alloy yolk-shell cubes exhibit much improved catalytic activity and durability compared with the commercial Pt/C catalysts. Given the facile synthesis, it is expected that the Cu_2O yolk-shell cube template method will open a new avenue for the development of novel catalysts with high electrocatalytic activity and durability.

Acknowledgements

This work was supported by NSFC (21073240 and 51173212), Natural Science Foundation of Guangdong Province (S2013020012833), Fundamental Research Fund for the Central Universities (13lgpy51), Fund of New Star Scientist of Pearl River Science and Technology of Guangzhou (2011J2200057), SRF for ROCS, SEM ([2012]1707).

Notes and references

1 F. Cheng, J. Shen, B. Peng, Y. Pan, Z. Tao and J. Chen, *Nature Chem.*, 2010, **3**, 79.
2 R. Wang, C. Wang, W. Cai and Y. Ding, *Adv. Mater.*, 2010, **22**, 1845.
3 Q. Chen, Z.-Y. Zhou, F. J. Vidal-Iglesias, J. Solla-Gullón, J. M. Feliu and Sun, S.-G. *J. Am. Chem. Soc.*, 2011, **133**, 12930.
4 C.-H. Cui, H.-H. Li and S.-H. Yu, *Chem. Sci.*, 2011, **2**, 1611.
5 H. Yang, *Angew. Chem. Int. Ed.*, 2011, **50**, 2674.
6 L. Wang and Y. Yamauchi, *J. Am. Chem. Soc.*, 2013, **135**, 16762.
7 H. Ataee-Esfahani, M. Imura and Y. Yamauchi, *Angew. Chem. Int. Ed.*, 2013, **52**, 13611.

8 C. Li, T. Sato and Y. Yamauchi, *Angew. Chem. Int. Ed.*, 2013, **52**, 8050.
9 R. H. Wang, Y. Xie, K. Y. Shi, J. Q. Wang, C. G. Tian, P. K. Shen and H. G. Fu, *Chem-Eur. J.*, 2012, **18**, 7443.
10 L. Wang and Y. Yamauchi, *J. Am. Chem. Soc.*, 2010, **132**, 13636.
11 F. Hong, S. Sun, H. You, S. Yang, J. Fang, S. Guo, Z. Yang, B. Ding, X. Song, *Cryst. Growth Des.*, 2011, **11**, 3694.
12 Y. Jia, Y. Jiang, J. Zhang, L. Zhang, Q. Chen, Z. Xie and L. Zheng, *J. Am. Chem. Soc.*, 2014, **136**, 3748.
13 F. Saleem, Z. Zhang, B. Xu, X. Xu, P. He and X. Wang, *J. Am. Chem. Soc.*, 2013, **135**, 18304.
14 H.-H. Li, S. Zhao, M. Gong, C.-H. Cui, D. He, H.-W. Liang, L. Wu and S.-H. Yu, *Angew. Chem. Int. Ed.*, 2013, **52**, 7472.
15 X.-S. An, Y.-J. Fan, D. Chen, Q. Wang, Z.-Y. Zhou and S.-G. Sun, *Electrochim. Acta*, 2011, **56**, 8912.
21 B. Y. Xia, H. B. Wu, X. Wang and X. W. Lou, *J. Am. Chem. Soc.*, 2012, **134**, 13934.
22 R. Iyyamperumal, L.Zhang, G. Henkelman and R. M. Crooks, *J. Am. Chem. Soc.*, 2013, **135**, 5521.
23 S. Chen, Z. Wei, X. Qi, L. Dong, Y.-G. Guo, L. Wan, Z. Shao and L. Li, *J. Am. Chem. Soc.*, 2012, **134**, 13252.
24 L. Zhang, N. Li, F. Gao, L. Hou and Z. Xu, *J. Am. Chem. Soc.*, 2012, **134**, 11326.
25 B. Y. Xia, H. Wu, X. Wang and X. W. Lou, *Angew. Chem. Int. Ed.*, 2013, **52**, 12337.
26 B. Y. Xia, W. T. Ng, H. B. Wu, X. Wang and X. W. Lou, *Angew. Chem. Int. Ed.*, 2012, **51**, 7213.
27 C. Hu, H. Cheng, Y. Zhao, Y. Hu, Y. Liu, L. Dai and L. Qu, *Adv. Mater.*, 2012, **24**, 5493.
28 J. Lee, J. C. Park and H. Song, *Adv. Mater.*, 2008, **20**, 1523.
29 S. Wu, J. Dzubiella, J. Kaiser, M. Drechsler, X. Guo, M. Ballauff and Y. Lu, *Angew. Chem. Int. Ed.*, 2012, **51**, 2229.
30 Z. W. Seh, W. Li, J. J. Cha, G. Zheng, Y. Yang, M. T. McDowell, P.-C. Hsu and Y. Cui, *Nature Commun.*, 2013, **4**, 1331.
31 J. Liu, S. Z. Qiao, S. B. Hartono and G. Q. Lu, *Angew. Chem. Int. Ed.*, 2010, **49**, 4981.
32 C.-H. Kuo, Y. Tang, L.-Y. Chou, B. Sneed, C. N. Brodsky, Z. Zhao and C.-K. Tsung, *J. Am. Chem. Soc.*, 2012, **134**, 14345.
33 Y. Yang, X. Liu, X. Li, J. Zhao, S. Bai and J. Liu, Q. Yang, *Angew. Chem. Int. Ed.*, 2012, **51**, 9164.
34 C.-H. Kuo, Y. Tang, L.-Y. Chou, B. T. Sneed, C. N. Brodsky, Z. Zhao and C.-K. Tsung, *J. Am. Chem. Soc.*, 2012, **134**, 14345.
35 J. Gao, G. Liang, J. Cheung, Y. Pan, Y. Kuang, F. Zhao, B. Zhang, X. Zhang, E. Wu and B. Xu, *J. Am. Chem. Soc.*, 2008, **130**, 11828.
36 M. Siegfried and K.-S. Choi, *Angew. Chem. Int. Ed.*, 2005, **117**, 3282.
37 J. P. Espinos, J. Morales and A. Barranco, *J. Phys.Chem. B*, 2002, **106**, 6921.
38 Z. Sun, X. Wang, Z. Liu, H. Zhang, P. Yu and L. Mao, *Langmuir*, 2010, **26**, 12383.